IEEE Access
Multidisciplinary | Rapid Review | Open Access Journal

Received January 8, 2021, accepted January 16, 2021, date of publication January 25, 2021, date of current version February 10, 2021.

Digital Object Identifier 10.1109/ACCESS.2021.3054178

Nonlinear Adaptive Robust Precision Pointing Control of Tank Servo Systems

SHUSEN YUAN[1], WENXIANG DENG[1,2], YAOWEN GE[1], JIANYONG YAO[1], (Member, IEEE), AND GUOLAI YANG[1]

[1]School of Mechanical Engineering, Nanjing University of Science and Technology, Nanjing 210094, China
[2]State Key Laboratory of Fluid Power and Mechatronic Systems, Zhejiang University, Hangzhou 310027, China

Corresponding author: Wenxiang Deng (wxdeng_njust@163.com)

This work was supported in part by the National Natural Science Foundation of China under Grant 51905271 and Grant 52075262, in part by the Natural Science Foundation of Jiangsu Province under Grant BK20190459, in part by the Fundamental Research Funds for the Central Universities under Grant 30920041101, and in part by the Open Foundation of the State Key Laboratory of Fluid Power and Mechatronic Systems under Grant GZKF-201910.

ABSTRACT This paper focuses on the high performance pointing control of tank servo systems with parametric uncertainties and uncertain nonlinearities including nonlinear friction, backlash and structural flexibility. A comprehensive dynamic nonlinear mathematical model of the two-DOF tank servo system is established. Specifically, to accurately describe the nonlinear friction characteristics in actual systems, a continuous friction model is employed. Moreover, a hybrid nonlinear model combining structural flexibility and transmission backlash is constructed to characterize the nonlinear characteristics of the backlash and flexible coupling between the input and output shafts of the drive end for the tank servo system. By using the backstepping method, a nonlinear adaptive robust controller is presented. In the controller, the adaptive law is compounded to dispose of parametric uncertainties and a well-designed continuous nonlinear robust control law is developed for the purpose of coping with unmodeled disturbances. The closed-loop system stability analysis indicates that the presented controller achieves an asymptotic tracking performance with parametric uncertainties and ensures the robustness against unmodeled disturbances theoretically. The effectiveness of the proposed control strategy is verified by a large number of comparative simulation results.

INDEX TERMS Tank servo systems, nonlinearity, uncertainty, adaptive control, robust control.

I. INTRODUCTION

Tank servo systems are significant parts of modern tank fire control systems [1]. They are mainly used to realize the azimuth and pitch attitude adjustment and servo tracking of the tank guns. Meanwhile the servo system is also a key factor to ensure the stability of the tank turrets and guns while the tanks are moving. However, the tank servo system not only has many complex nonlinear factors, but also includes parametric uncertainties and unmodeled disturbances. The high precision pointing control for tank servo systems has always been the focus of control scholars and engineering experts. Although the controllers based on linear control theory are currently relatively mature, their global stability and servo tracking performance can hardly meet the current requirements [2]. Therefore, it is indispensable to further explore progressive nonlinear control strategies to improve high performance for tank servo systems.

To improve the pointing control performance of tank servo systems, the current research mainly focuses on the following two aspects: the precise modeling of tank servo systems and the improvement of control strategies. The traditional control methods for the tank servo systems are mainly based on a single-channel independent design, which consider the movement of the azimuth subsystem and the pitch subsystem to be independent. Meanwhile the design of the controllers was mainly aimed at the independent research of the relevant characteristics for the motors in the subsystem, ignoring the dynamic characteristics of the tank servo system. In [3]–[6], by designing different nonlinear control methods to enhance the tracking performance for the tank servo systems, it was essentially the control of servo motors for azimuth or pitch subsystems. The design of the above controllers has not considered the two-axis dynamic coupling characteristics, which will lead to not good enough control performance.

The associate editor coordinating the review of this manuscript and approving it for publication was Zheng Chen.

This work is licensed under a Creative Commons Attribution 4.0 License. For more information, see https://creativecommons.org/licenses/by/4.0/

In [7], [8], the two-axis dynamic coupling models of the tank servo systems were established, and the corresponding controllers were designed, however, the electrical dynamics were not taken into consideration, which makes the designed control law not suitable for practical application. In [9], a dynamic model of two-DOF tank servo system with two motor drive subsystems was established. However, the friction nonlinearity, model uncertainty and dynamic characteristics of servo motors were not deeply explored.

In addition to the two-axis coupling characteristics, the friction, backlash, flexibility and mechanism nonlinearity in the tank servo systems are all obstacles to our accurate modeling process. How to unify the above nonlinearities in the form of mathematical representation plays a significant role in improving the performance for the designed controller. Friction nonlinearity is a key factor affecting the low-speed servo performance of the systems [10]. Accurate friction compensation can availably boost the servo performance for the tank servo systems. The influence of friction nonlinearity was not considered in some control studies for tank servo systems [11], [12]. Most studies consider the effect of friction nonlinearity when designing controllers, but the friction model was considered a simple Stribeck model [13], [14]. However, it should be noted that the Stribeck friction model is piecewise continuous, which means it is not differentiable. It is conflicting to design a controller based on the backstepping method to deal with unmatched nonlinear frictions through the traditional Stribeck model. Hence, there is still room for improvement of the friction nonlinearity in the design process of the previous tank servo system controllers.

Furthermore, the impact of backlash and flexible nonlinearity in the tank servo system cannot be ignored [15], and related scholars had done in-depth research on it from the structure [16], [17] and control theory [9], [18]–[21]. The theoretical analysis of the backlash nonlinearity for the tank servo system provided a basis for the design of nonlinear compensation control strategies [18], [19]. In [20], an adaptive robust controller was designed for the backlash nonlinearity in the tank servo system. In [9], an optimal control scheme was derived for backlash compensation. On the basis of [9], the backlash and flexible nonlinearity were combined into consideration for tank servo system, used optimal control designs for backlash compensation and flexible nonlinearity was handled by feedback linearization.

In the dynamic systems with small moment of inertia and low speed of the controlled object, the flexible nonlinearity can generally be ignored [22], [23]. However, in the tank servo systems, flexible nonlinearity will cause the systems to lag significantly and form mechanical resonance. In the launching state of tank moving, all transmission shafts (including motor shafts), gears on the shafts, fasteners, couplings, and transmission boxes and bases of the transmission devices all have different degrees of elastic deformation [24]. Therefore, the flexible nonlinear analysis of the tank servo systems is quite complicated. To simplify the research difficulty, generally the flexibility of the entire transmission device can be equivalent to the output shaft [9], [24], [25]. The flexibility of the transmission shaft between the motor and the load was represented by a linear spring model for tank servo systems [9], [24]–[27]. In [26], through parameter identification of the transmission shaft stiffness coefficient, the flexible nonlinearity of the tank servo system was further studied.

Moreover, apart from the dynamic coupling and nonlinear characteristics mentioned above, there are also many model uncertainties, which can be divided into parameter uncertainties and unmodeled disturbances, in the tank servo systems [24], [25]. The parameter uncertainties are mainly reflected in the change of load mass and coefficient of viscous friction. The unmodeled disturbances include dynamic characteristics of the system and external disturbances which cannot be accurately considered during modeling. In [28], [29], the unmodeled disturbances of the tank servo system were estimated by the extended state observer. In [30], the RBF neural network was used to adaptively approximate the system perturbation parameters and unmodeled disturbances to suppress the chattering of the system. In [31], [32], the authors proposed σ modification and normalization signal methods for the simultaneous existence of unmodeled dynamics and bounded disturbance. For the external disturbance and parameter uncertainty in the tank servo system, a control scheme combining disturbance observer and sliding mode variable structure control was proposed [33]. Obviously, the above research dealt with the model uncertainties for tank servo systems in the design process of the controllers, which improved the servo performance of the systems compared with the traditional PID controller.

In this paper, a nonlinear adaptive robust controller is put forward for high performance pointing control of tank servo systems come under parametric uncertainties and uncertain nonlinearities including nonlinear friction, backlash and structural flexibility based on backstepping method. In the controller design, the parameter adaptation law is integrated to reduce the parametric uncertainties, and the unmodeled disturbances are handled by certain robust feedback. The system friction nonlinearity is described by a continuous differentiable friction model, including viscous friction, coulomb friction and Stribeck effect. The unknown parameters in the friction model are updated by adaptation law to achieve accurate friction compensation. A hybrid nonlinear model combining structural flexibility and transmission backlash is constructed to describe the nonlinear characteristics of the backlash and flexible coupling between the input and output shafts of the drive end for the tank servo system. Due to the feedforward cancellation, the adverse effects caused by the system nonlinearities are much alleviated. The action paths of various feedforward compensation strategies are considered in combination with the nonlinear coupling characteristics of the azimuth subsystem motors and the pitch subsystem electric cylinder. In the design of the final feedforward control law, decoupling control of various nonlinear factors is realized through full state feedback. The proposed nonlinear

adaptive robust controller not only guarantees the asymptotic tracking performance for parametric uncertainties, but also has good robustness to unmodeled disturbances.

The main contributions of this paper include the following aspects. 1) A comprehensive nonlinear dynamic mathematical model of tank servo system is built considering the two-axis coupling dynamic characteristics, nonlinear friction, backlash, transmission shaft flexibility, as well as various model uncertainties, including parameter uncertainties and unmodeled disturbances. 2) A model-based nonlinear adaptive robust control strategy is proposed to achieve high-precision pointing control of tank servo systems.

3) When the projection-type adaptive law is adopted, the stability of the closed-loop system will not be disturbed, the mutual influence between parameter adaptation and robust control law can be reduced, and the gain setting efficiency of the controller is improved. 4) To test the proposed controller, extensive comparative simulation results are acquired to demonstrate its superiority and availability.

This paper is arranged as follows. Chapter II gives the formulation of the problem and the dynamic models. Chapter III introduces the design process of the presented nonlinear adaptive robust controller and its primary theoretical consequence. Comparative simulation consequences are achieved from chapter IV. Chapter V gives some conclusions.

II. PROBLEM FORMULATION AND DYNAMIC MODELS

The main function of the tank servo system in the movement of the tank is reflected in the following two aspects. Aim at the angle of the tank gun barrel while the tank is moving. After the angle aiming, the tank gun is kept in a stable state to improve the first shot hit rate. The subsystems of tank gun barrel in the process of tank firing can be divided into azimuth subsystem and pitch subsystem. The goal is that given a sequential control input, the tank servo system as far as possible to track any smooth motion trajectory.

A. NONLINEAR DYNAMIC MODEL OF TANK SERVO SYSTEM

The two-axis coupling system diagram of the tank servo system based on the [9] is shown in Figure 1. The characteristics of the two-axis coupling structure of the tank servo system as well as the characteristics in the process of firing are described in Figure 1. The angle change of the barrel in the pitch subsystem and the turret in the azimuth subsystem describes the position of the barrel in the working space for the tank servo system.

According to the analysis of traditional robot modeling technology in [34], the dynamic model of tank servo systems is derived. To make the modeling and derivation process concise and clear, in the tank servo system the tank turret is referred to as part 1, and the tank gun is referred to as part 2.

The azimuth rotation angle of tank gun and the pitch rotation angle of tank gun were defined $q = \begin{bmatrix} q_1 & q_2 \end{bmatrix}^T \in R^2$, the corresponding angular velocity $\dot{q} = \begin{bmatrix} \dot{q}_1 & \dot{q}_2 \end{bmatrix}^T \in R^2$.

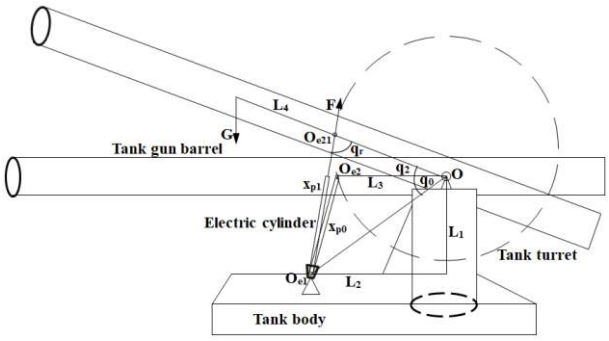

FIGURE 1. Two-axis coupling system diagram of the tank servo system.

According to the Euler–Lagrange dynamics equation, the mathematical model of the coupling nonlinear dynamics for the tank servo system is built as follows:

$$M_a(q)\ddot{q} + M_b(q, \dot{q})\dot{q} - \delta_g = T \tag{1}$$

where $Ma(q)$ is a positive definite symmetric generalized mass matrix, $M_b(q)$ is a Coriolis matrix; δ_g is gravity vector of the conservative force system of the tank servo system, $\delta_g = \begin{bmatrix} \delta_{g1} & \delta_{g2} \end{bmatrix}^T = \begin{bmatrix} 0 & -m_2 g L_4 \cos q_2 \end{bmatrix}^T \in R^2$, δ_{g1} represents the gravitational moment of the azimuth subsystem, δ_{g2} represents the gravitational moment of the pitch subsystem; m_2 represents the mass of the barrel for the azimuth subsystem; L_4 is the distance between the trunnion of the tank gun and the centroid of the barrel; $T = \begin{bmatrix} T_1 & T_2 \end{bmatrix}^T \in R^2$, T_1 is the driving torque at the load end of the tank azimuth subsystem, T_2 is the driving torque at the load end of the tank pitch subsystem.

B. MATHEMATICAL MODEL OF THE DRIVE END OF THE AZIMUTH SUBSYSTEM

The tank azimuth subsystem mainly controls the movement of the turret in horizontal direction, which is mainly composed of power converter, turret motor, current sensor, directional machine, horizontal gyroscope and horizontal controller.

Considering the friction characteristics and the unmodeled disturbance of the driving end of the azimuth subsystem, the load-end torque balance equation in the azimuth direction can be written as

$$T_1 = T_{m1} - f_1(\dot{q}_1) - d_1(t). \tag{2}$$

The tank azimuth subsystem is driven by a servo motor via a reducer, there are inevitably problems with transmission backlash and structural flexibility. Therefore, the torque balance equation of the azimuth subsystem is:

$$T_{m1} = G_1(\varphi(q_{m1}/n_1) - q_1) \tag{3}$$

where T_{m1} is the torque at the end of the drive shaft after considering the flexibility of the drive shaft; $f_1(\dot{q}_1)$ is the friction torque of the azimuth subsystem; d_1(t) is the unmodeled disturbance in the azimuth subsystem; $\varphi(q_{m1}/n_1)$ is a function describing the transmission backlash; q_{m1} is the

rotation angle of the azimuth subsystem motor; n_1 represents the reduction ratio of the azimuth subsystem motor; G_1 is the stiffness coefficient of the transmission shaft.

The friction characteristics have a greater impact on the low-speed performance of the azimuth subsystem, in order to more accurately describe the true friction behavior, the following continuous nonlinear friction model [35] is adopted:

$$f_1(\dot{q}_1) = l_{11}\left[tanh(c_{11}\dot{q}_1) - \tanh(c_{12}\dot{q}_1)\right] + l_{12}\tanh(c_{13}\dot{q}_1) + l_{13}\dot{q}_1 \quad (4)$$

where l_{11}, l_{12}, l_{13} are different friction levels; c_{11}, c_{12}, c_{13} are different shape coefficients that characterize the friction characteristics; Without viscous dissipation, the Coulomb friction coefficient exists and is modeled through the term $l_{12}\tanh(c_{13}\dot{q}_1)$; the term $\tanh(c_{11}\dot{q}_1) - \tanh(c_{12}\dot{q}_1)$ is the Stribeck effect and the term $l_{13}\dot{q}_1$ denotes the viscous friction.

The servo motor at the drive end of the azimuth subsystem adopts a three-closed-loop control structure. Since the electrical response is much faster than the mechanical response, the drive speed loop can be approximated as a first-order inertia link. The first-order inertia link can be used to describe the relationship between the angular velocity of the azimuth servo motor and the control input. Hence, the dynamics of the motor system can be expressed as follows:

$$\ddot{q}_{m1} = \frac{b_{p1}}{\tau_{p1}}u_1 - \frac{1}{\tau_{p1}}\dot{q}_{m1} + \Delta_1(t) \quad (5)$$

where b_{p1} is the steady-state gain of the velocity loop of the azimuth subsystem, τ_{p1} is the time constant of the approximate model of the first-order inertia link of the velocity loop for the azimuth subsystem, u_1 is the control input of the azimuth subsystem, $\dot{q}_{m1}$ is the angular velocity of the motor for the azimuth subsystem, $\ddot{q}_{m1}$ is the angular acceleration of the azimuth subsystem with respect to the motor, $\Delta_1(t)$ represents the approximate model error at the drive end of the azimuth subsystem.

C. MATHEMATICAL MODEL OF THE DRIVE END OF THE PITCH SUBSYSTEM

The pitch subsystem is mainly composed of the power converter, the servo motor, the ball screw, the current sensor, the high-low direction gyroscope and the high-low direction controller.

The kinematics schematic diagram of the pitching subsystem is shown in Figure 1. The difference between the modeling and azimuth subsystem lies in the modeling of the electric cylinder. The inner part of the electric cylinder adopts a gear reducer and a ball screw for transmission, which converts the linear motion into the rotary motion of the tank barrel. Due to the fast response, the high transmission efficiency, easy maintenance, long life and other characteristics of the electric cylinder. The use of electric cylinders as power sources is a very important part of the all-electric tanks in China.

In Figure 1, O is the tank gun trunnion; O_{e1} is the lower fulcrum of the electric cylinder, O_{e2} is the upper fulcrum of the electric cylinder, L_1 is the vertical distance from the tank gun trunnion to the lower fulcrum of the electric cylinder, L_2 is the horizontal distance from the tank gun trunnion to the lower fulcrum of the electric cylinder, L_3 is the distance from the trunnion of the tank gun to the upper fulcrum of the electric cylinder, L_4 is the distance from the tank gun trunnion to the center of mass of the barrel. x_{p0} is the initial length of the electric cylinder, x_{p1} is the length of the electric cylinder after adjusting the gun angle (the length between the point O_{e1} and the point O_{e21}), $\Delta(x)$ represents the push rod displacement of the electric cylinder piston.

Considering the friction characteristics of the driving end and the unmodeled disturbances of the pitching subsystem, the load-end torque balance equation of the pitching subsystem can be expressed as:

$$T_2 = F \cdot L_3 \sin q_r - m_2.g \cdot L_4 \cos q_2 - f_2(\dot{q}_2) - d_2(t) \quad (6)$$

where F is the output thrust of the electric cylinder, q_r is the angle between the output thrust of the electric cylinder and the axis of the barrel, q_2 is the pitch angle of the barrel, $f_2(\dot{q}_2)$ is the friction torque of the pitch subsystem, $d_2(t)$ is the unmodeled disturbance of the pitch subsystem.

In order to characterize the real friction behavior more accurately, the following continuous nonlinear friction model [35] $f_2(\dot{q}_2)$ is used

$$f_2(\dot{q}_2) = l_{21}\left[tanh(c_{21}\dot{q}_2) - \tanh(c_{22}\dot{q}_2)\right] + l_{22}\tanh(c_{23}\dot{q}_2) + l_{23}\dot{q}_2 \quad (7)$$

where l_{21}, l_{22}, l_{23} are different friction levels; c_{21}, c_{22}, c_{23} are different shape coefficients that characterize the friction characteristics; Without viscous dissipation, the Coulomb friction coefficient exists and is modeled through the term $l_{22}\tanh(c_{23}\dot{q}_2)$; the term $\tanh(c_{21}\dot{q}_2) - \tanh(c_{22}\dot{q}_2)$ is the Stribeck effect and the term $l_{23}\dot{q}_2$ denotes the viscous friction.

Since there is a corresponding nonlinear relationship between the push rod displacement of the electric cylinder and the rotation angle of the tank barrel, the following trigonometric function relationship can be obtained according to the figure 1: $q_0 = \arctan(\frac{L_1}{L_2})$, $x_{p0} = \sqrt{(L_2 - L_3)^2 + L_1^2}$, $\sin qr = \frac{\sqrt{L_1^2+L_2^2}sin(q_2+q_0)}{x_{p1}}$, $x_{p1} = \sqrt{L_3^2 + L_1^2 + L_2^2 - 2L_3\sqrt{L_1^2 + L_2^2}\cos(q_0 + q_2)}$, $\Delta x = x_{p1} - x_{p0} = \frac{l}{2\pi n_2}q_{m2}$.

Similar to the azimuth subsystem, the tank pitch system also has problems with transmission backlash and structural flexibility. Therefore, the torque at the end of the motor drive shaft of the pitch subsystem can be expressed as:

$$T_{m2} = G_2(\varphi(q_{m2}/n_2) - q_2) \quad (8)$$

where G_2 is the stiffness coefficient of the transmission shaft; n_2 is the reduction ratio of the pitch subsystem reducer; q_{m2} is the rotation angle of the pitch subsystem motor; $\dot{q}_{m2}$ is the rotational angular velocity of the pitch subsystem motor.

The relationship between the output thrust and torque of the ball screw is as follows:

$$T_{m2} = \frac{l}{2\pi\eta}F \tag{9}$$

where l is the lead of the ball screw, η is the mechanical efficiency of the screw.

The servo motor at the drive end of the pitch subsystem also adopts a three-closed-loop control structure. Similar to the azimuth subsystem, the drive speed loop can be approximated as a first-order inertia link. The dynamics of the motor system is expressed as:

$$\ddot{q}_{m2} = \frac{b_{p2}}{\tau_{p2}}u_2 - \frac{1}{\tau_{p2}}\dot{q}_{m2} + \Delta_2(t) \tag{10}$$

where b_{p2} is the steady-state gain of the velocity loop of the pitch subsystem, τ_{p2} is the time constant of the approximate model of the first-order inertia link of the velocity loop of the pitch subsystem, u_2 is the control input of the pitch subsystem, $\ddot{q}_{m2}$ is the angular acceleration of the motor of the pitch subsystem, $\Delta_2(t)$ represents the approximate model error at the drive end of the pitch subsystem.

III. NONLINEAR ADAPTIVE ROBUST CONTROLLER DESIGN

A. DESIGN MODEL AND ISSUES TO BE ADDRESSED

According to the formula (1), (2), (5), (6) and (10), the torque balance equation of the tank servo system can be derived:

$$M_a(q)\ddot{q} = W_1 q_m - W_2 q - M_b(q,\dot{q})\dot{q} - T_f - W_3 - d(t) \tag{11}$$

$$\ddot{q}_m = W_4 u - W_5 \ddot{q}_m + \Delta(t) \tag{12}$$

where

$$M_a(q) = \begin{bmatrix} A_{11}(q) & A_{12}(q) \\ A_{21}(q) & A_{22}(q) \end{bmatrix},$$

$$M_b(q) = \begin{bmatrix} 0 & B_{12}(q\ \dot{q}) \\ B_{21}(q\ \dot{q}) & B_{22}(q\ \dot{q}) \end{bmatrix}, W_1 = \begin{bmatrix} \frac{G_1}{n_1} & 0 \\ 0 & \frac{2\pi\eta G_2}{l n_2}h(x_{12}) \end{bmatrix},$$

$$W_2 = \begin{bmatrix} G_1 & 0 \\ 0 & \frac{2\pi\eta G_2}{l}h(x_{12}) \end{bmatrix}, W_3 = \begin{bmatrix} 0 \\ m_2 g L_4 \cos(x_{12}) \end{bmatrix},$$

$$W_4 = \begin{bmatrix} \frac{b_{p1}}{\tau_{p1}} & 0 \\ 0 & \frac{b_{p2}}{\tau_{p2}} \end{bmatrix}, W_5 = \begin{bmatrix} \frac{1}{\tau_{p1}} & 0 \\ 0 & \frac{1}{\tau_{p2}} \end{bmatrix}, q = \begin{bmatrix} q_1\ q_2 \end{bmatrix}^T,$$

$$q_m = \begin{bmatrix} q_{m1}\ q_{m2} \end{bmatrix}^T, T = \begin{bmatrix} T_1\ T_2 \end{bmatrix}^T, T_f = \begin{bmatrix} f_1(\dot{q}_1)\ f_2(\dot{q}_2) \end{bmatrix}^T,$$

$$d(t) = \begin{bmatrix} d_1(t)\ d_2(t) \end{bmatrix}^T, \Delta(t) = \begin{bmatrix} \Delta_1(t)\ \Delta_2(t) \end{bmatrix}^T,$$

$$h(x_{12}) = L_3 \sin q_r = \frac{L_3\sqrt{L_1^2 + L_2^2}sin(q_2 + q_0)}{x_{p1}}.$$

Aiming at the problems of transmission gap and structural flexibility in the tank servo system, take the azimuth subsystem as an example. Let $y_1 = q_{1m}/n_1$, then the gap function $\varphi(y_1) = \varphi(q_{1m}/n_1)$ can be processed as follows:

$$\varphi(y_1) = y_1 + d_1(y_1) \tag{13}$$

where $d_1(y_1) = d_{11}(y_1) + d_{12}(y_1)$, $d_{11}(y_1) = [\varphi_0 - y_{10}]e^{-\alpha(y_1 - y_{10})sign(\dot{y}_1)}$, $d_{12}(y_1) = e^{-\alpha y_1 sign(\dot{y}_1)}\int_{y_{10}}^{y_1}[b-1]e^{\alpha v sign(\dot{y}_1)}dv$, both parameter α and parameter b are constants; $d_1(y_1)$ is bounded as shown in [36]; $\varphi(y_1)$ can represent the effect of the backlash; G_i is the stiffness coefficient of the transmission shaft. Therefore, the influence of the flexibility of the transmission shaft and the nonlinearity of the transmission gap can be expressed based on the equations (3) and (8).

Define the following state variables as $x_1 = [x_{11}x_{12}]^T = [q_1 q_2]^T$, $x_2 = [x_{21}x_{22}]^T = [\dot{q}_1\dot{q}_2]$, $x_3 = [x_{31}\ x_{32}]^T = [q_{m1}\ q_{m2}]^T$, $x_4 = [x_{41}\ x_{42}]^T = [\dot{q}_{m1}\dot{q}_{m2}]^T$, then the tank servo system can be expressed in a state-space form as

$$\begin{cases} \dot{x}_1 = x_2 \\ M_a(x_1)\dot{x}_2 = W_1 x_3 - W_2 x_1 \\ \quad - M_b(x_1, x_2)x_2 - T_f - W_3 - d(t) \\ \dot{x}_3 = x_4 \\ \dot{x}_4 = W_4 u - W_5 x_4 + \Delta(t) \end{cases} \tag{14}$$

Generally, Due to the changes in the movement state of the tank during the journey, the friction characteristics of the azimuth and pitch rotation axis of the servo system will change accordingly, resulting in changes in the corresponding parameters of the tank servo system, such as l_{11}, l_{12}, l_{13}, l_{21}, l_{22} and l_{23}. Therefore, the unknown parameters are defined as $\theta = [\theta_1, \theta_2, \theta_3]^T$, where $\theta_1 = [\theta_{11}, \theta_{21}]^T$, $\theta_2 = [\theta_{12}, \theta_{22}]^T$, $\theta_3 = [\theta_{13}, \theta_{23}]^T$ and $\theta_{11} = l_{11}$, $\theta_{12} = l_{12}$, $\theta_{13} = l_{13}$, $\theta_{21} = l_{21}$, $\theta_{22} = l_{22}$, $\theta_{23} = l_{23}$. Based on the equations (4) and (7), relevant parameters in the continuous nonlinear friction model are defined as follows:

$$\varphi(x_2) = [\varphi_1(x_2), \varphi_2(x_2), \varphi_3(x_2)]^T,$$

$$\varphi_1(x_2) = \begin{bmatrix} \tanh(c_1\dot{q}_1) & 0 \\ 0 & \tanh(c_1\dot{q}_2) \end{bmatrix},$$

$$\varphi_2(x_2) = \begin{bmatrix} \tanh(c_2\dot{q}_1) - \tanh(c_3\dot{q}_1) & 0 \\ 0 & \tanh(c_2\dot{q}_2) - \tanh(c_3\dot{q}_2) \end{bmatrix},$$

$$\varphi_3(x_2) = \begin{bmatrix} \dot{q}_1 & 0 \\ 0 & \dot{q}_2 \end{bmatrix}.$$

Hence, the state-space form (14) is able to be rewritten as follows

$$\begin{cases} \dot{x}_1 = x_2 \\ M_a(x_1)\dot{x}_2 = W_1 x_3 - W_2 x_1 - M_b(x_1, x_2)x_2 \\ \qquad\qquad - \varphi(x_2)^T\theta - W_3 - d(t) \\ \dot{x}_3 = x_4 \\ \dot{x}_4 = W_4 u - W_5 x_4 + \Delta(t) \end{cases}. \tag{15}$$

Before the controller design, the following assumption is made.

Assumption 1: The desired position trajectory $x_{1d}(t) \in C^4$ and bounded;

Assumption 2: The defined unknown parameters satisfy

$$\theta \in \Omega_\theta\{\theta :\ \theta_{\min} \le \theta \le \theta_{\max}\} \tag{16}$$

where $\theta_{\min} = [\theta_{11\min}, \theta_{21\min}, \theta_{12\min}, \theta_{22\min}, \theta_{13\min}, \theta_{23\min}]^T$, $\theta_{\max} = [\theta_{11\max}, \theta_{21\max}, \theta_{12\max}, \theta_{22\max}, \theta_{13\max}, \theta_{23\max}]^T$ are known.

Assumption 3: The unmodeled disturbance $d(t)$ and the approximate model error $\Delta(t)$ in (15) are bounded, i.e.,

$$|d(t)| \leq \delta_1, \Delta(t) \leq \delta_2 \tag{17}$$

where δ_1 and δ_2 are unknown constants.

B. PROJECTION MAPPING AND PARAMETER ADAPTATION

Let $\hat{\theta}$ denotes the estimate of unknown parameter θ and $\tilde{\theta}$ denotes the estimation error (i.e $\tilde{\theta} = \hat{\theta} - \theta$). Viewing (16), a discontinuous projection can be described as [37]:

$$\Pr oj_{\hat{\theta}i}(\bullet i) = \begin{cases} 0, \ if \ \hat{\theta}_i = \theta_{i\max} \ and \ \bullet i > 0 \\ 0, \ if \ \hat{\theta}_i = \theta_{i\min} \ and \ \bullet i < 0 \\ \bullet i, \ otherwise \end{cases} \tag{18}$$

where $\bullet i$ describes the ith component from the vector $\bullet$, the action $<$ for two vectors is executed according to the corresponding elements of the vectors. The $i = 11, 21, 12, 22, 13, 23$. By applying an adaptation law presented by

$$\dot{\hat{\theta}} = \Pr oj_{\hat{\theta}} (\Gamma\tau) \ with \ \theta_{\min} \leq \hat{\theta}(0) \leq \theta_{\max} \tag{19}$$

where $\Gamma > 0$ represents a diagonal adaptation rate matrix and τ represents an adaptation function after synthesis. For arbitrary adaption function τ, the projection mapping employed in (19) ensures

$$(P1)\hat{\theta} \in \Omega_{\hat{\theta}} \left\{ \hat{\theta} : \ \theta_{\min} \leq \hat{\theta} \leq \theta_{\max} \right\} \tag{20}$$

$$(P2)\tilde{\theta}^T \left[\Gamma^{-1} \Pr oj_{\hat{\theta}}(\Gamma\tau) - \tau \right] \leq 0, \forall\tau. \tag{21}$$

C. CONTROLLER DESIGN

Step 1: Designing the adaptive robust controller according to the backstepping method [37]–[39] because the design model (15) contains unmatched uncertainties. Before designing the controller we first need to define the following error variables

$$z_2 = \dot{z}_1 + k_1 z_1 = x_2 - x_{2eq} \tag{22}$$

$$x_{2eq} = \dot{x}_{1d} - k_1 z_1, z_3 = x_3 - \alpha_2, z_4 = x_4 - \alpha_3 \tag{23}$$

where $z_1 = x_1 - x_{1d}$ is the output tracking error; x_{2eq} is the virtual control law of the state x_2; z_2 represents the discrepancy between the actual state x_2 and the virtual control x_{2eq}; and k_1 is a positive feedback gain; α_2 is the virtual control law of the state x_3; z_3 is the discrepancy between the actual state x_3 and the virtual control α_2; α_3 is the virtual control law of the state x_4; z_4 is the discrepancy between the actual state x_4 and the virtual control α_3.

On account of the transfer function between z_1 and z_2 is able to be expressed as $G(s) = z_1(s)\, z_2(s) = 1/(s + k_1)$, which is a steady transfer function. If the tracking error z_1 becomes small or converges to zero then z_2 gets small or converges to zero. Therefore, how to make z_2 smaller is the next main design goal.

Step 2: Considering the equation (15) and the equation (22), the derivative of z_2 with respect to time is

$$\begin{aligned} M_a(x_1)\dot{z}_2 &= M_a(x_1)\dot{x}_2 - M_a(x_1)\dot{x}_{2eq} \\ &= W_1 x_2 - W_2 x_1 - M_b(x_1, x_2)x_2 - \varphi^T(x_2)\theta \\ &\quad -W_3 - d(t) - M_a(x_1)\dot{x}_{2eq} \end{aligned} \tag{24}$$

By combining the definition of error z_3, there can be

$$\begin{aligned} M_a(x_1)\dot{z}_2 &= M_a(x_1)\dot{x}_2 - M_a(x_1)\dot{x}_{2eq} \\ &= W_1 z_3 + W_1\alpha_2 - W_2 x_1 - M_b(x_1, x_2)x_2 \\ &\quad -\varphi^T(x_2)\theta - W_3 - d(t) - M_a(x_1)\dot{x}_{2eq}. \end{aligned} \tag{25}$$

In this step, the analysis shows that the state x_3 can be regarded as a virtual control input, and the α_2 is designed for x_3. Thus, the virtual control law α_2 is

$$\begin{aligned} \alpha_2 &= \alpha_{2a} + \alpha_{2s}, \ \alpha_{2s} = \alpha_{2s1} + \alpha_{2s2}, \\ \alpha_{2s1} &= -W_1^{-1} k_2 z_2, \\ \alpha_{2a} &= W_1^{-1}[W_2 x_1 + M_b(x_1, x_2)x_2 \\ &\quad +\varphi(x_2)\hat{\theta} + W_3 + M_a(x_1)\dot{x}_{2eq}]. \end{aligned} \tag{26}$$

In (26), k_2 is a positive feedback gain; α_{2a} is a model-based adaptive feedforward compensation control law, which can enhance the tracking accuracy of the system; α_{2s} is the robust control law where α_{2s1} is the linear robust feedback term for stabilizing the nominal tank servo system and α_{2s2} is a nonlinear robust control law used to refrain from the unmodeled disturbance. In order to stabilize the system, α_{2s2} is designed to satisfy the following stabilization conditions:

$$z_2 \left[\alpha_{2s2} + \varphi(x_2)^T \tilde{\theta} - d(t) \right] \leq \xi_1 \tag{27}$$

$$z_2 \alpha_{2s2} \leq 0. \tag{28}$$

Hence the robust term α_{2s2} is described as

$$\alpha_{2s2} = W_1^{-1} \frac{-h_1}{2\xi_1} z_2 \tag{29}$$

where ξ_1 is a positive design parameter which can be arbitrarily small, and h_1 is any smooth function meeting the following definitions:

$$h_1 \geq \|\varphi\|^2 \|\theta_M\|^2 + \delta_1^2 \tag{30}$$

where $\theta_M = \theta_{\max} - \theta_{\min}$.

Substituting (26) into (25), we obtain

$$M_a(x_1)\dot{z}_2 = W_1 z_3 + \varphi(x_2)\tilde{\theta} - d(t) - k_2 z_2 + \alpha_{2s2}. \tag{31}$$

From the analysis of the equation (31), it can be seen that if $z_3 = 0$, the nonlinear robust control law α_{2s2} can refrain from the unmodeled disturbance $d(t)$, and the synthesized adaptive law can deal with the uncertainty of parameters, so the expected output tracking can be achieved through the follow-up stability analysis. Hence, in the next step, the goal is to make the z_3 as small as possible.

Step 3: Combining the equation (23) and calculating the time derivative of the error z_3 can be obtained

$$\dot{z}_3 = \dot{x}_3 - \dot{\alpha}_2 = x_4 - \dot{\alpha}_2 = z_4 + \alpha_3 - \dot{\alpha}_2 \tag{32}$$

where $\dot{\alpha}_2$ will be divided into two parts: the known and calculable part is represented by $\dot{\alpha}_{2c}$ which will be applying in the controller design; the incalculable and unknown part is represented by $\dot{\alpha}_{2u}$ which will be refrained from certain robust feedback, then

$$\begin{aligned}\dot{\alpha}_{2c} = &\frac{\partial \alpha_2}{\partial x_1} x_2 + \frac{\partial \alpha_2}{\partial x_2} M_a^{-1}(x_1)[W_1 x_3 - W_2 x_1 \\ &- M_b(x_1, x_2) x_{23} - \varphi(x_2)^T \hat{\theta}] - W + \frac{\partial \alpha_2}{\partial \hat{\theta}} \dot{\hat{\theta}} + \frac{\partial \alpha_2}{\partial t}\end{aligned} \tag{33}$$

$$\dot{\alpha}_{2u} = \frac{\partial \alpha_2}{\partial x_2} M_a^{-1}(x_1) \left[\varphi(x_2)^T \tilde{\theta} + d(t)\right]. \tag{34}$$

The virtual control law α_3 will be designed as follows:

$$\alpha_3 = \alpha_{3a} + \alpha_{3s}, \ \alpha_{3s} = \alpha_{3s1} + \alpha_{3s2} \tag{35}$$

$$\alpha_{3a} = \dot{\alpha}_{2c}, \ \alpha_{3s1} = -k_3 z_3 \tag{36}$$

where k_3 is a positive feedback gain; α_{3a} is a model-based adaptive feedforward compensation control law, which can improve the tracking accuracy of the system; α_{3s} is the robust control law where α_{3s1} is a linear robust feedback term for stabilizing the nominal tank servo system and α_{3s2} is a nonlinear robust control law used to refrain from the unmodeled disturbance. In order to stabilize the system, α_{3s2} is designed to satisfy the following stabilization conditions:

$$z_3 [\alpha_{3s2} - \dot{\alpha}_{2u}] \leq \xi_2 \tag{37}$$

$$z_3 \alpha_{3s2} \leq 0. \tag{38}$$

Hence the robust term α_{3s2} is designed as

$$\alpha_{3s2} = \frac{-h_2}{2\xi_2} z_3 \tag{39}$$

where ξ_2 is a positive design parameter which is able to be arbitrarily small, h_2 is any smooth function meeting the following conditions

$$\begin{aligned}h_2 \geq &\left\| \frac{\partial \alpha_2}{\partial x_2} \right\|^2 \left\| M_a^{-1}(x_1) \right\|^2 \|\varphi(x_2)\|^2 \|\theta_M\|^2 \\ &+ \left\| \frac{\partial \alpha_2}{\partial x_2} \right\|^2 \left\| M_a^{-1}(x_1) \right\|^2 \delta_1^2\end{aligned} \tag{40}$$

Substituting the formulas (36) and (37) into (33), we have

$$\dot{z}_3 = z_4 - k_3 z_3 + \alpha_{3s2} - \dot{\alpha}_{2u}. \tag{41}$$

Step 4: In this step the actual control law for u will be proposed. Considering the equations (15) and (23), differentiating z_4 with respect to time, then

$$\dot{z}_4 = \dot{x}_4 - \dot{\alpha}_3 = W_4 u - W_5 x_4 + \Delta(t) - \dot{\alpha}_3 \tag{42}$$

where $\dot{\alpha}_3 = \dot{\alpha}_{3c} + \dot{\alpha}_{3u}$, $\dot{\alpha}_{3c} = \frac{\partial \alpha_3}{\partial x_1} x_2 + \frac{\partial \alpha_3}{\partial x_2} \dot{x}_2 + \frac{\partial \alpha_3}{\partial \hat{\theta}} \dot{\hat{\theta}} + \frac{\partial \alpha_3}{\partial t}$ is the known and computable part which will be applied in the controller design; $\dot{\alpha}_{3u} = \frac{\partial \alpha_3}{\partial x_2} M_a^{-1}(x_1) \left[\varphi(x_2)^T \tilde{\theta} + d(t)\right]$ is the unknown and incalculable part which will be suppressed by certain robust feedback.

According to the structure of (42), on account of the adaptive robust design program [40]–[42], the ARC controller can be obtained through

$$u = u_a + u_s, u_s = u_{s1} + u_{s2} \tag{43}$$

$$u_a = W_4^{-1}[W_5 x_4 + \dot{\alpha}_{3c}], u_{s1} = W_4^{-1}(-k_4 z_4) \tag{44}$$

where k_4 is a positive feedback gain. In (44), u_a is an adjustable feedforward control law which is employed to achieve an improved model compensation through parameter adaptation (19); u_s is a robust control law where u_{s1} is a linear robust feedback law for stabilizing the nominal model of the system and u_{s2} is a nonlinear robust term to handle the approximate model error in (42).

In order to the robust design, we set the robust term u_{s2} as arbitrarily continuous function that satisfies the following conditions:

$$z_4 [u_{s2} + \Delta(t) - \dot{\alpha}_{3u}] \leq \zeta_3 \tag{45}$$

$$z_4 u_{s2} \leq 0 \tag{46}$$

where ξ_3 is a positive design parameter that can be any arbitrarily small. Based on (42), the robust term u_{s2} is designed as

$$u_{s2} = -\frac{h_3}{2\xi_3} z_4 \tag{47}$$

where h_3 is an arbitrary smooth function according with the following conditions:

$$\begin{aligned}h_3 \geq &\left(\left\| \frac{\partial \alpha_2}{\partial x_2} \right\| \left\| M_a^{-1}(x_1) \right\| \|\varphi(x_2)\| \|\theta_M\| \right. \\ &\left. + \left\| \frac{\partial \alpha_2}{\partial x_2} \right\| \left\| M_a^{-1}(x_1) \right\| \delta_1 \right)^2 + \delta_2^2\end{aligned} \tag{48}$$

Substituting the resulting ARC controller u into (42), we have

$$\dot{z}_4 = -k_4 z_4 + u_{s2} + \Delta(t) - \dot{\alpha}_{3u}. \tag{49}$$

D. MAIN RESULTS

Theorem 1: If the unmodeled disturbance $d(t) = 0$ and the approximate model error $\Delta(t) = 0$, the system only exists backlash nonlinearity, flexible nonlinearity of the transmission shaft and parametric uncertainties of the nonlinear frictions. According to the projection type adaptation law (19), then the adaptation function can be achieved as $\tau = \frac{\partial \alpha_2}{\partial x_2} M_a^{-1}(x_1) \varphi(x_2) z_3 + \frac{\partial \alpha_3}{\partial x_2} M_a^{-1}(x_1) \varphi(x_2) z_4 - \varphi(x_2) z_2$ and selecting feedback gains k_1, k_2, k_3 and k_4 large enough such that the following defined matrix Λ is positive definite, (50), as shown at the bottom of the next page

Hence, the presented control law (43) ensures the following two aspects, the boundedness of all signals in the closed-loop system and the asymptotic output tracking performance, i.e., $z_1 \to 0$ as $t \to \infty$.

Proof: See Appendix A.

Remark 1: It is clear from the theorem that, in the presence of parametric uncertainties, unmodeled disturbances, friction,

backlash and flexible nonlinearity of the transmission shaft, the presented controller achieves perfect asymptotic tracking performance and tracking error converges to zero. In addition, increasing the gains k_1, k_2, k_3 and k_4 can enhanced the convergence rate. This asymptotic output tracking performance can effectively improve the high performance motion control of the tank servo system.

Theorem 2: If the unmodeled disturbance $d(t) \neq 0$ and the approximate model error $\Delta(t) \neq 0$, then the presented control law (43) ensures the boundedness of all signals in the closed-loop system, and the Lyapunov function which is positive definite expressed as follows

$$V_2(t) = \frac{1}{2}z_1^T z_1 + \frac{1}{2}M_a(x_1)z_2^T z_2 + \frac{1}{2}z_3^T z_3 + \frac{1}{2}z_4^T z_4 \quad (51)$$

is bounded by

$$V_2(t) \leq V_2(0)\exp(-\vartheta t) + \frac{\xi}{\vartheta}[1 - \exp(-\vartheta t)] \quad (52)$$

where $\xi = \xi_1 + \xi_2 + \xi_3$, $\vartheta = 2\lambda_{\min}(\Lambda) min\left\{1, M_a^{-1}(x_1), 1, 1\right\}$, $\lambda_{\min}(\Lambda)$ represents the minimum eigenvalue of Λ.

Proof: See Appendix B.

Remark 2: It is shown from Theorem 2 that even when the tank servo system contains unmodeled disturbance and approximate model error, the proposed adaptive controller also guarantees the tracking error to be bounded. Simultaneously, the (52) shows that the transient performance and the final tracking error can be adjusted freely by certain controller parameters in a foregone form: the ϑ is the converging rate which can be arbitrarily large, and $\frac{\xi}{\vartheta}$, the bound of $V(\infty)$ (the index of the final tracking errors), can be made wantonly small through augmenting gains k_1, k_2, k_3 and k_4 and/or reducing controller parameters ξ_1, ξ_2 and ξ_3.

IV. COMPARATIVE SIMULATION RESULTS

In order to fully verify the accuracy of the nonlinear comprehensive dynamic model for coupling loads between axes of tank servo system established in this paper, and the availability of the adaptive robust controller designed. In the simulation, the following four controllers are used for comparison.

1) ARC: This is the adaptive robust controller (43) presented in this paper. The system parameters are: $A_{11}(q) = 2547 + 5400\cos^2(q_2) - 2\sin(q_2)\rangle\cos(q_2) + 224\sin^2(q_2)$, $A_{12}(q) = A_{21}(q) = 2.8\cos(q_2) + 13.7\sin(q_2)$, $A_{22}(q) = 5443$, $B_{12}(q) = [10350\cos(q_2)\sin(q_2) + 1.5(\cos^2(q_2) - \sin^2(q^2))]\dot{q}_1 - (13.7\cos(q_2) - 2.8\sin(q_2))\dot{q}_2$, $B_{21}(q) = -2B_{12}(q)$, $B_{22}(q) = [1.5\sin(q_2) - 6.8\cos(q_2)]\ \dot{q}_1$, $h_1 = 0.6$m, $h_3 = 5$m; the driving end of the azimuth subsystem parameters are $L_{m1} = 0.05$H, $R_{m1} = 2.6\Omega$, $k_{u1} = 1.11$N.m/A, $J_{m1} = 1.16 \times 10^{-4}$kg.m^2, $G_1 = 5 \times 10^6$N/m, $n_1 = 200$, $K_{e1} = 0.64$ V.s/rad; the driving end of the pitch subsystem parameters are $L_{m2} = 0.0107$H, $R_{m2} = 1.93\Omega$, $k_{u2} = 0.55$N.m/A, $J_{m2} = 6.04 \times 10^{-4}$kg.m^2, $n_2 = 550$, $K_{e2} = 0.5$V.s/rad, $G_2 = 5 \times 10^6$N/m, $L_1 = 0.5$m, $L_2 = 2.8$m, $L_3 = 1.2$m, $L_4 = 4.5$m, $l = 0.025$m, $m_2 = 200$kg, $\eta = 0.85$. The control gains are set as: $k_{11} = 100$, $k_{21} = 10$, $k_{31} = 1000$, $k_{41} = 1$, $k_{12} = 200$, $k_{22} = 200000$, $k_{32} = 10$, $k_{42} = 500$. The initial estimate of θ is given as $\hat{\theta}(0) = [200, 100, 50, 200, 100, 50]^T$. Parameter adaptation rates are selected as $\Gamma = diag\{62.5, 0.6, 1.7, 182, 6.7, 45\}$.

2) PI: This is a traditional proportional-integral controller. The controller gains carefully adjusted by the trail-and-error method are $K_{p1} = 90000$, $K_{i1} = 300$ and $K_{p2} = 60000$, $K_{i2} = 300$.

3) AC: This is the conventional adaptive controller which neglects the unmodeled disturbance $d(t)$ and the approximate model error $\Delta(t)$. There is no discrepancy between the AC and the ARC except that it has no nonlinear robust control law. To insure that the comparison between them is quite enough, the AC controller and the ARC controller select the same control gains.

4) FLC: This is the feedback linearization controller. The main difference between it and the AC controller is that there is no parameter adaptation. The parameter adaptation rates in the FLC are given as their primary values, i.e., $\hat{\theta} = \hat{\theta}(0)$ and $\Gamma = 0$. The remaining controller parameters of FLC are no different from the corresponding parameters of the ARC controller. The method can testify the availability of the parameter adaptation law integrated from this paper.

To effectively compare the quality of each controller, based on the tracking errors the following three evaluation indices maximum Me, average μ, and standard deviation σ [43] are applied to assess the quality of each control arithmetic.

The four controllers are first tested for a smooth normal motion trajectory, i.e., in which the azimuth subsystem and the pitch subsystem are respectively: $x_{1d1}(t) = 0.5\arctan[1 - e^{-t^3}]$ rad and $x_{1d2}(t) = 0.25\arctan[1 - e^{-t^3}]$ rad.

TABLE 1. Performance indices during the whole time history for azimuth subsystem.

Indices	*Me*	μ	σ
ARC	0.0071	0.00147	0.00133
PI	0.0549	0.00783	0.01531
FLC	0.0852	0.00898	0.01920
AC	0.0112	0.00223	0.00212

$$\Lambda = \begin{bmatrix} k_1 - \frac{1}{2}I & 0 & 0 & 0 \\ 0 & k_2 - \frac{1}{2}I - \frac{1}{2}\|W_1\|I - \frac{1}{2}\left\|\dot{M}_a(x_1)\right\|I & 0 & 0 \\ 0 & 0 & k_3 - \frac{1}{2}\|W_1\|I - \frac{1}{2}I & 0 \\ 0 & 0 & 0 & k_4 - \frac{1}{2}I \end{bmatrix} \quad (50)$$

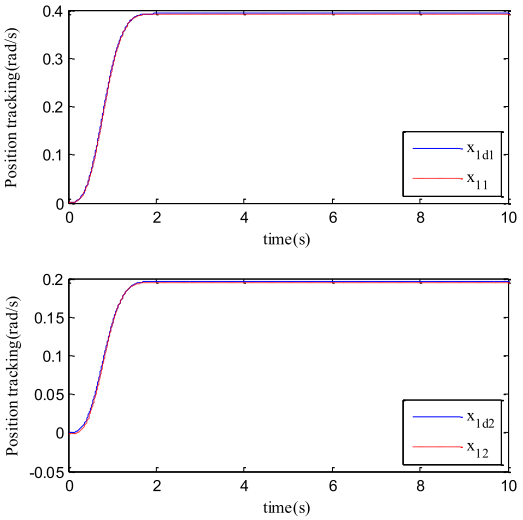

FIGURE 2. Position tracking of ARC for azimuth subsystem and pitch subsystem.

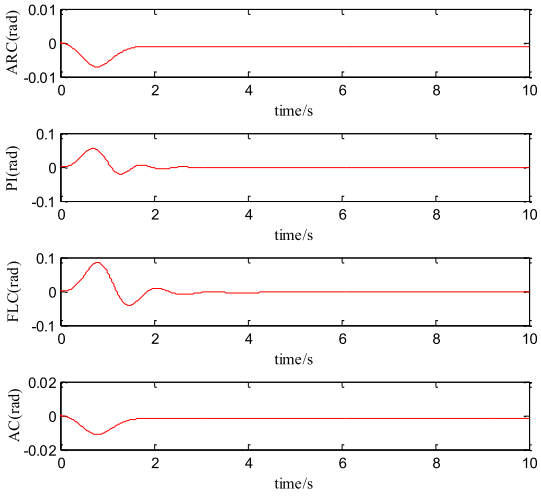

FIGURE 3. Compared tracking errors for azimuth subsystem.

TABLE 2. Performance indices during the whole time history for pitch subsystem.

Indices	*Me*	μ	σ
ARC	0.0011	0.00062	0.00013
PI	0.0240	0.00278	0.00582
FLC	0.0333	0.00333	0.00778
AC	0.0043	0.00236	0.00057

The performance of controller ARC based on azimuth subsystem and pitch subsystem is shown in Figure 2 respectively. The tracking performance of the four controllers for the azimuth subsystem and the pitch subsystem are shown in Figures 3-4 respectively. Tables 1-2 respectively collect the performance indexes of the four controllers compared in the whole cycles, which can clearly reflect their tracking performance. Whether it is the azimuth subsystem or the pitch

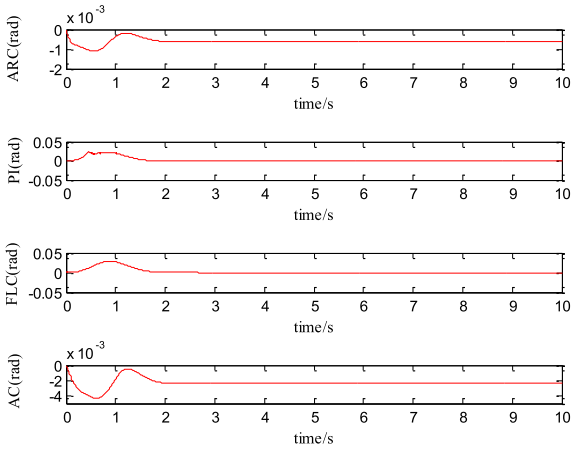

FIGURE 4. Compared tracking errors for pitch subsystem.

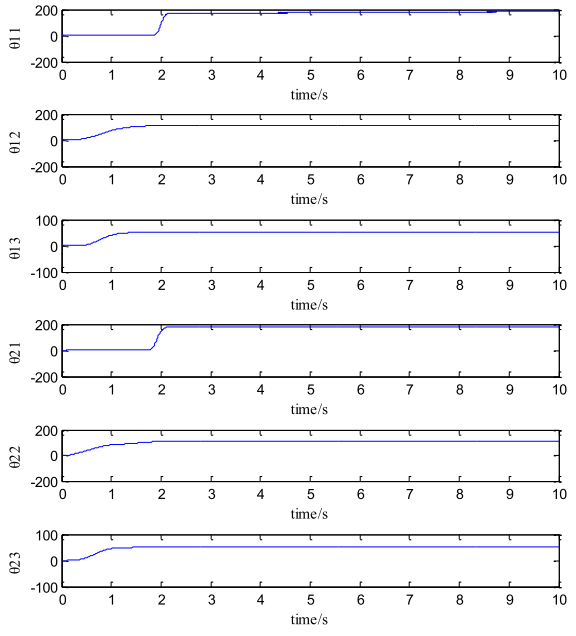

FIGURE 5. Friction level parameter adaptation of ARC for normal motion.

subsystem, all the results show that the designed ARC controller is feasible and is better than the other three controllers in terms of transient and final tracking error. By comparing the tracking effects of the ARC and AC controllers, it can be found that the nonlinear robust control law has a non-negligible effect on the performance of the controller. This is why the ARC controller is superior to the AC, and it also verifies the anti-interference capacity of the nonlinear robust term for the ARC controller. It can be found from the Figures 3-4 that the tracking error of the FLC controller is larger than the AC controller because the advantage of the AC controller lies in the use of flexible model compensation through parameter adaptation. Therefore, the availability of the synthetic adaptive laws in the article is verified. The effect of the PI is better than that of the FLC, which is the effect of the stronger feedback gain of the PI. However, the tracking

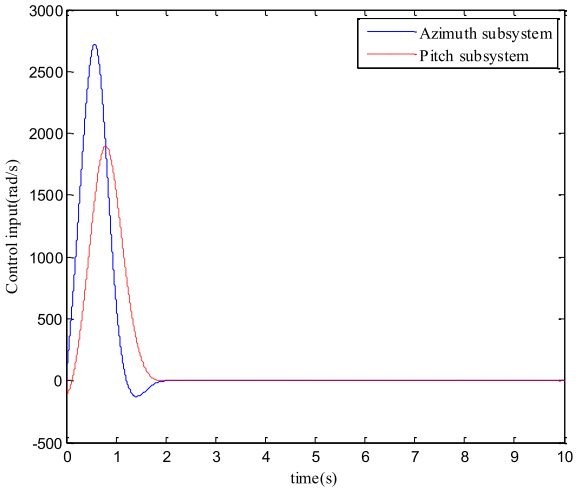

FIGURE 6. Control input of azimuth subsystem and pitch subsystem.

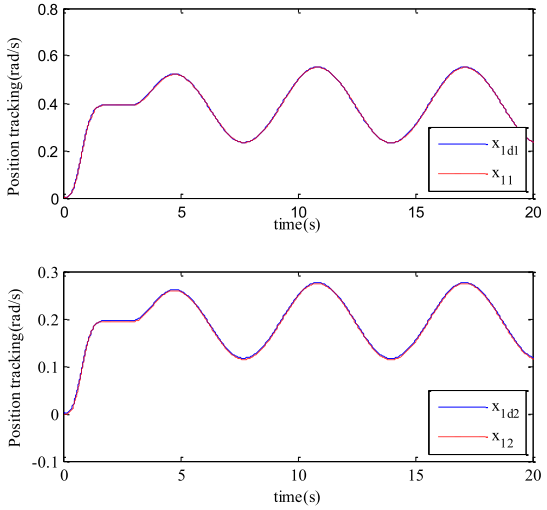

FIGURE 7. Comparative position tracking of ARC for azimuth subsystem and pitch subsystem.

TABLE 3. Performance indices during the whole time history for azimuth subsystem.

Indices	*Me*	μ	σ
ARC	0.0071	0.00175	0.00171
PI	0.0548	0.00806	0.01096
FLC	0.0851	0.01348	0.01813
AC	0.0112	0.00271	0.00269

performance of the ARC and the AC perfectly surpasses the PI, which illustrates the superiority of the design method based on the nonlinear model. The convergence of parameter estimation of ARC is presented in Figure 5. The control input of azimuth subsystem and pitch subsystem for the ARC controller are shown in Figure 6. They are all regular, bounded and continuous.

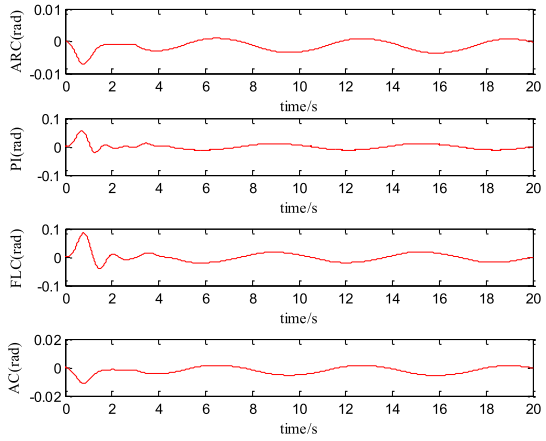

FIGURE 8. Compared tracking errors for azimuth subsystem.

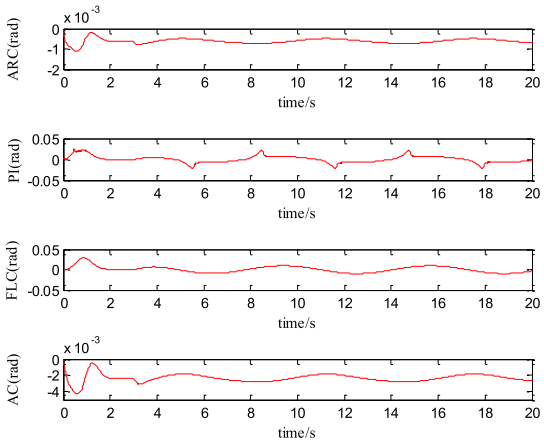

FIGURE 9. Compared tracking errors for pitch subsystem.

TABLE 4. Performance indices during the whole time history for pitch subsystem.

Indices	*Me*	μ	σ
ARC	0.0011	0.00061	0.00012
PI	0.0240	0.00629	0.00809
FLC	0.0289	0.00641	0.00797
AC	0.0043	0.00233	0.00052

To further verify the dynamic tracking performance of the ARC controller proposed in this paper, the position tracking of the ARC controller of the azimuth subsystem and the pitch subsystem are shown in Figure 7 respectively. The main difference is that they are gradually switched to sinusoidal instructions after 3 seconds, i.e., $0.8\sin(t-3)\left[1-e^{-(t-3)}\right]$rad and $0.4\sin(t-3)\left[1-e^{-(t-3)}\right]$rad, which better reflect the dynamic tracking performance of the proposed control strategy. The comparative tracking errors are presented in Figure 8 and Figure 9 respectively. The performance indexes of the azimuth subsystem and the pitch subsystem for whole cycles are given in Table 3 and Table 4. Visible, the ARC controller proposed in this paper still

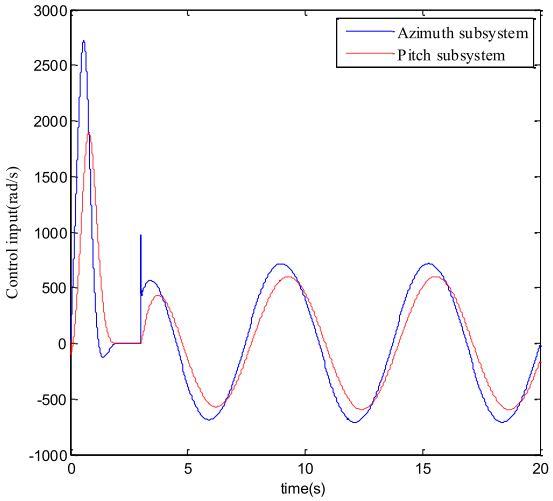

FIGURE 10. Control input of azimuth subsystem and pitch subsystem.

achieves the most perfect tracking performance in all performance indicators. For the azimuth subsystem and the pitch subsystem, FLC has obtained more unsatisfactory tracking performance than AC. This further testifies the superiority of the parameter adaptation law for the tank servo system. The PI controller still exceeds FLC in every system with its formidable feedback gain. By comparing the results of ARC and AC, it can be found that ARC eliminates the adverse effects of the gap nonlinearity, friction nonlinearity, and drive shaft flexibility nonlinearity of the tank servo system with the nonlinear robust control law, and obtains better tracking performance. The control input of azimuth subsystem and pitch subsystem for the ARC controller are presented in Figure 10 which are all inerratic, bounded and continuous. Under different motion conditions, it can be clearly found that there is a certain difference between the Figure 6 and Figure 10, which is mainly due to the change of control input caused by the different motion states of the tank servo system.

V. CONCLUSION

In this paper, an adaptive robust controller is proposed for high performance precision pointing control of tank servo system with dynamic coupling nonlinearity between linkage parts, frictional nonlinearities, backlash nonlinearities, drive shaft flexible nonlinearities, nonlinearity of the mechanism in the electric cylinder, parametric uncertainties and unmodeled disturbances. Based on the established comprehensive dynamic model of tank servo system, the continuous differentiable friction model is adopted to compensate the friction nonlinearities reasonably and effectively. A nonlinear model of structural flexibility and transmission backlash is constructed to describe the nonlinear characteristics considering the backlash and flexible coupling between the input and output axes of tank servo systems. Combining with the size of the articulated mechanism of the electric cylinder, the nonlinear relationship between the displacement of the electric push rod and the rotation angle of the tank barrel is established. Parametric uncertainties are disposed via adaptive laws integrated in the backstepping design and unmodeled disturbances are handled by certain robust feedback. The stability of the closed-loop system is guaranteed by the Lyapunov method, which shows that the proposed controller can achieve asymptotic tracking performance in the presence of parameter uncertainties and multiple nonlinearities, and also ensures that robustness of the existing unmodeled disturbances and approximate modeling errors. Comparative simulation results have been achieved to illustrate the effectiveness of the presented control strategy.

As future works, it is of great significance to think out the advantages of adaptive robust controllers in output feedback forms for tank servo systems. In addition, because the tank servo system is a complex electromechanical coupling system, designing a model-based control strategy requires high precision modeling, the model free control strategies [44] can be introduced in future research, which is more suitable for practical application.

APPENDIX A

Proof of Theorem 1: In this case, define $d(t) = \left[d_1(t)\ d_2(t)\right]^T = \left[0\ 0\right]^T$, $\Delta(t) = \left[\Delta_1(t)\ \Delta_2(t)\right]^T = \left[0\ 0\right]^T$,and consider the following Lyapunov function:

$$V_1 = \frac{1}{2}z_1^T z_1 + \frac{1}{2}M_a(x_1)z_2^T z_2 + \frac{1}{2}z_3^T z_3 + \frac{1}{2}z_4^T z_4 + \frac{1}{2}\tilde{\theta}^T\Gamma^{-1}\tilde{\theta} \tag{A1}$$

Based on (22), (35), (41), (49), then we can have

$$\begin{aligned}\dot{V}_1 = {} & z_1^T(z_2 - k_1 z_1) + z_2^T(W_1 z_3 + \varphi(x_2)\tilde{\theta} - k_2 z_2) + \frac{1}{2}\dot{M}_a(x_1) \\ & \cdot z_2^T z_2 + z_3^T(z_4 - k_3 z_3 - \dot{\alpha}_{2u}) + z_4^T(-k_4 z_4 - \dot{\alpha}_{3u}) \\ & + \tilde{\theta}^T\Gamma^{-1}\dot{\hat{\theta}}\end{aligned} \tag{A2}$$

Integrating its definition and property from (35) according to the adaptation function τ, we can set the upper bound (A2) as

$$\begin{aligned}\dot{V}_1 \le {} & |z_1|\,|z_2| - k_1 z_1^2 + W_1\,|z_2|\,|z_3| - k_2 z_2^2 \\ & + \frac{1}{2}\dot{M}_a(x_1)z_2^2 + |z_3|\,|z_4| - k_3 z_3^2 - k_4 z_4^2 \\ \le {} & -(k_1 - \frac{1}{2}I)z_1^2 - (k_2 - \frac{1}{2}I - \frac{1}{2}W_1 I - \frac{1}{2}\dot{M}_a(x_1)I)z_2^2 \\ & -(k_3 - \frac{1}{2}W_1 I - \frac{1}{2}I)z_3^2 - (k_4 - \frac{1}{2}I)z_4^2\end{aligned} \tag{A3}$$

Noting the defined matrix Λ is positive definite, then the upper bound according to the above equation (A3) can be written as

$$\dot{V}_1 \le -z^T\Lambda z \le -\lambda_{\min}(\Lambda)z^T z = -W < 0 \tag{A4}$$

where $z = [|z_1|, |z_2|, |z_3|, |z_4|]^T$, $\lambda_{min}(\Lambda)$ represents the minimum eigenvalue of the matrix Λ and W is a positive function. Therefore, $V_1 \in L_\infty$, $W \in L_2$ and the error signals z are bounded. From the assumption 1, it can be derived that x is bounded. From assumption 2 and assumption 3, we can guarantee that all the estimated parameters are bounded,

and deduce that the control input u is bounded. Hence, all signals in the closed-loop system are bounded. According to the equation (22), (31), (41), (49) can verify that the time derivative of W is bounded, which also indicates that W is uniformly continuous. Employing *Barbalat's* lemma [43], $W \to 0$ as $t \to \infty$, which generates the results in Theorem 1.

APPENDIX B

Proof of Theorem 2: If the system includes time-variant unmodeled disturbances and approximate modeling errors, $d(t) = \left[d_1(t)\ d_2(t)\right]^T \neq \left[0\ 0\right]^T$, $\Delta(t) = \left[\Delta_1(t)\ \Delta_2(t)\right]^T \neq \left[0\ 0\right]^T$, the time derivative of V_2 defined in (51) is

$$\begin{aligned}\dot{V}_2 = {} & z_1^T(z_2 - k_1 z_1) + z_2^T(W_1 z_3 + \varphi(x_2)\tilde{\theta} + \alpha_2 s_2 - d(t) \\ & -k_2 z_2) + \frac{1}{2}\dot{M}_a(x_1) z_2^T z_2 + z_3^T(z_4 - k_3 z_3 \\ & +\alpha_3 s_2 - \dot{\alpha}_{2u}) + z_4^T(-k_4 z_4 + u_{s2} - \dot{\alpha}_{3u} + \Delta(t)) \quad \text{(B1)}\end{aligned}$$

Then we can make the following reasonable derivation:

$$\begin{aligned}\dot{V}_2 \leq {} & |z_1|\,|z_2| - k_1 z_1^2 + W_1\,|z_2|\,|z_3| - k_2 z_2^2 + |z_2|\,(\varphi(x_2)\tilde{\theta} \\ & +\alpha_2 s_2 - d(t)) + \frac{1}{2}\dot{M}_a(x_1) z_2^2 + |z_3|\,|z_4| - k_3 z_3^2 \\ & +|z_3|\,(\alpha_3 s_2 - \dot{\alpha}_{2u}) - k_4 z_4^2 + |z_4|\,(u_{s2} - \dot{\alpha}_{3u} + \Delta(t)). \quad \text{(B2)}\end{aligned}$$

Based on the equations (27), (37), (45), we can upper bound (B2) as

$$\dot{V}_2 \leq -z^T \Lambda z + \xi. \quad \text{(B3)}$$

Considering that the matrix Λ is positive definite, so

$$\dot{V}_2 \leq -\lambda_{\min}(\Lambda)(z_1^2 + z_2^2 + z_3^2 + z_4^2) + \xi \leq -\vartheta V_2 + \xi. \quad \text{(B4)}$$

which will lead to (52) by applying the comparison lemma [43]. Hence, the error signal z is bounded. Similar to the proof of Theorem 1, the boundedness of all signals can be deduced to prove.

REFERENCES

[1] T. Dursun, F. Büyükcivelek, and Ç. Utlu, "A review on the gun barrel vibrations and control for a main battle tank," *Defence Technol.*, vol. 13, no. 5, pp. 353–359, Oct. 2017.
[2] H. E. Merritt, *Hydraulic Control Systems*. New York, NY, USA: Wiley, 1967.
[3] L. A. Pars, *A Treatise on Analytical Dynamics*. New York, NY, USA: Wiley, 1965.
[4] Q. Gao, R. Hou, G. Yang, B. Mao, and Y. Hou, "Adjustment and control of a certain top-mounted gun based on a novel fractional order neural sliding mode strategy," *Acta Armamentarii*, vol. 34, no. 10, pp. 1311–1317, 2013.
[5] Q. Yang, Q. Yan, J. Cai, J. Tian, and X. Guan, "Neural network-based error-tracking iterative learning control for tank gun control systems with arbitrary initial states," *IEEE Access*, vol. 8, pp. 72179–72187, 2020.
[6] C. Sun, J. Chen, L. Dou, and J. Tian, "Tank regulator design using unit vector control," *Trans. Beijing Inst. Technol.*, vol. 20, no. 5, pp. 593–596, 2000.
[7] L. Ye, Y. Xia, M. Fu, and C. Li, "Active disturbance rejection control for gun control of unmanned turret," *Control Theory Appl.*, vol. 31, no. 11, pp. 1580–1588, 2014.
[8] J. Tian, L. Qian, and R. Zhao, "Robust control of the axis of firepower pointing system," *J. Gun Launch Control*, vol. 1, pp. 61–64, 2011.
[9] G. Tao, X. Ma, and Y. Ling, "Optimal and nonlinear decoupling control of systems with sandwiched backlash," *Automatica*, vol. 37, no. 2, pp. 165–176, Feb. 2001.
[10] Q. Liu, L. Er, and J. Liu, "Overview of characteristics, modeling and compensation of nonlinear friction in servo systems," *J. Syst. Eng. Electron.*, vol. 24, no. 11, pp. 45–52, 2002.
[11] L. J. Shen, Y. Bao, and J. P. Cai, "Adaptive control of uncertain gun control system of tank," *Appl. Mech. Mater.*, vols. 88–89, pp. 88–92, Aug. 2011.
[12] L. Feng, X. Lei, and X. Ma, "Adaptive sliding mode robust control of gun control system of tank," *J. Gun Launch Control*, vol. 35, no. 10, pp. 55–58, 2010.
[13] Z. Zhu, C. Li, N. Li, and J. Zhang, "Study on adaptive friction compensation control of all-electric tank gun," *J. Gun Launch Control*, vol. 2, pp. 19–23, 2010.
[14] D. Yuan, X. Ma, W. Wei, and Y. Zhao, "Research on friction nonlinearity and low velocity performance of gun control system of tank," *J. Acad. Armored Force Eng.*, vol. 21, no. 4, pp. 57–61, 2007.
[15] H. Tao and J. Zhang, "Stability analysis of an automanual-propelled anti-aircraft weapon system," *Acta Armamentarii*, vol. 7, no. 1, pp. 28–32, 1986.
[16] G. Wang, X. Hou, and W. Wang, "The design and research of tank's traversing mechanism flexibility compensating device," *J. Armored Force Eng. Inst.*, vol. 17, no. 1, pp. 51–53, 2003.
[17] X. Chen, B. Li, Y. Liu, and Z. He, "Clearances identification of guns mechanism based on the second wavelet," *J. Vib. Shock*, vol. 27, no. S, pp. 348–350, 2008.
[18] K.-C. Li, "Modeling and compensation control analysis of backlash nonlinearity in gun control system of tanks," *Small Special Elect. Mach.*, vol. 38, no. 06, pp. 45–48, 2010.
[19] L.-J. Shen and J. P. Cai, "Adaptive robust control of gun control servo system of tank," *Math. Pract. Theory*, vol. 42, no. 7, pp. 170–175, 2012.
[20] D. Yuan, X. Ma, and S. Wei, "Modeling of nonlinearity and analysis on run performance for tank gun control system(II)," *J. Gun Launch Control*,vol. 31, no. 2, pp. 30–34, 2011.
[21] Y. Ling and G. Tao, "Numerical design and analysis of backlash compensation for a multivariable nonlinear tracking system," in *Proc. Amer. Control Conf.*, Jun. 1999, pp. 3539–3543.
[22] D. Li, "The influence of the servo system function by the elasticity deformation of the mechanism and the solutions," *China Heavy Equip.*, vol. 3, pp. 17–21, 2003.
[23] H. Wu, X. Yi, and K. Yang, "Mechanism structure factors on performance of opto-electronic tracker servo systems," *J. Appl. Opt.*, vol. 25, no. 3, pp. 11–14, 2004.
[24] X. Ma, F. Wang, and D. Yuan, "Nonlinearity characteristics and its control strategies of all-electric tank gun control system," *J. Acad. Armored Force Eng.*, vol. 25, no. 1, pp. 63–67 and 82, 2011.
[25] D. Yuan, X. Ma, S. Wei, X. Qiao, and Q. Liu, "Nonlinearity modelling and running performance analysis of tank gun control system(I)," *J. Gun Launch Control*, no. 4, pp. 32–36, 2010.
[26] D. Yuan and X. Ma, "Research on nonlinearity state estimation and parameter identification of tank gun control system," *Acta Armamentarii*, vol. 31, no. 8, pp. 1020–1025, 2010.
[27] D. Yuan, X. Ma, L. Li, and T. Liu, "Adaptive compensation control method of nonlinearity in tank gun control system based on equivalent disturbance," *J. Gun Launch Control*, vol. 36, no. 6, pp. 70–73, 2011.
[28] C. Wang, Y. Xia, M. Fu, and Z. Zhu, "Application of active disturbance rejection control in tank gun control system," in *Proc. IEEE 5th Int. Conf. Cybern. Intell. Syst.*, Sep. 2011, pp. 13–18.
[29] S. Yuan, J. Yao, W. Deng, G. Yang, and X. Ma, "Active disturbance rejection adaptive control of tank turret-gun control systems," in *Proc. 39th Chin. Control Conf. (CCC)*, Jul. 2020, pp. 333–339.
[30] J. Hu, Y. Hou, Q. Gao, Y. Chen, and Z. Tong, "Method of neural network adaptive sliding mode control of gun control system of tank," *J. Gun Launch Control*, vol. 43, no. 6, pp. 118–121 and 126, 2018.
[31] R. Ortega, L. Praly, and Y. Tang, "Direct adaptive tuning of robust controllers with guaranteed stability properties," *Syst. Control Lett.*, vol. 8, no. 4, pp. 321–326, Mar. 1987.
[32] G. Tao and P. A. Ioannou, "Robust adaptive control: A modified scheme," *Int. J. Control*, vol. 54, no. 1, pp. 241–256, 1991.
[33] H. Wang, Q. Wang, Z. Zuo, J. Qiao, and Y. Xia, "Sliding mode variable structure control for tank servo system based on disturbance observer," *J. Syst. Simul.*, vol. 21, no. 14, pp. 4487–4491, 2009.
[34] A. Bejczy, T. Tarn, and Y. Chen, "Robot arm dynamic control by computer," in *Proc. IEEE Int. Conf. Robot. Autom.*, Mar. 1985, pp. 960–970.
[35] G. Yang and J. Yao, "High-precision motion servo control of double-rod electro-hydraulic actuators with exact tracking performance," *ISA Trans.*, vol. 103, pp. 266–279, Aug. 2020.

[36] C.-Y. Su, Y. Stepanenko, J. Svoboda, and T. P. Leung, "Robust adaptive control of a class of nonlinear systems with unknown backlash-like hysteresis," *IEEE Trans. Autom. Control*, vol. 45, no. 12, pp. 2427–2432, Dec. 2000.
[37] B. Helian, Z. Chen, and B. Yao, "Precision motion control of a servo motor-pump direct drive electro-hydraulic system with a nonlinear pump flow mapping," *IEEE Trans. Ind. Electron.*, vol. 67, no. 10, pp. 8638–8648, Oct. 2020.
[38] M. Krstic, I. Kanellakopoulos, and P. V. Kokotovic, *Nonlinear and Adaptive Control Design*. New York, NY, USA: Wiley, 1995.
[39] W. Sun, S. Tang, H. Gao, and J. Zhao, "Two time-scale tracking control of nonholonomic wheeled mobile robots," *IEEE Trans. Control Syst. Technol.*, vol. 24, no. 6, pp. 2059–2069, Nov. 2016.
[40] G. Yang and J. Yao, "Output feedback control of electro-hydraulic servo actuators with matched and mismatched disturbances rejection," *J. Franklin Inst.*, vol. 356, no. 16, pp. 9152–9179, Nov. 2019.
[41] B. Yao and M. Tomizuka, "Adaptive robust control of SISO nonlinear systems in a semistrict feedback form," *Automatica*, vol. 33, no. 5, pp. 893–900, 1997.
[42] L. Lyu, Z. Chen, and B. Yao, "Advanced valves and pump coordinated hydraulic control design to simultaneously achieve high accuracy and high efficiency," *IEEE Trans. Control Syst. Technol.*, vol. 29, no. 1, pp. 236–248, Jan. 2021, doi: 10.1109/TCST.2020.2974180.
[43] J. Yao, Z. Jiao, and D. Ma, "Extended-state-observer-based output feedback nonlinear robust control of hydraulic systems with backstepping," *IEEE Trans. Ind. Electron.*, vol. 61, no. 11, pp. 6285–6293, Nov. 2014.
[44] W. Sun, X. Wang, and C. Zhang, "A model-free control strategy for vehicle lateral stability with adaptive dynamic programming," *IEEE Trans. Ind. Electron.*, vol. 67, no. 12, pp. 10693–10701, Dec. 2020.

SHUSEN YUAN received the B.Tech. degree in rail transportation signal and control from Jiangsu Normal University, Xuzhou, China, in 2018. He is currently pursuing the Ph.D. degree with the School of Mechanical Engineering, Nanjing University of Science and Technology, Nanjing, China.

His current research interests include servo control of mechatronic systems and adaptive robust control.

WENXIANG DENG received the B.Tech. degree in mechanical engineering from Central South University, Changsha, China, in 2013, and the Ph.D. degree in mechanical engineering from the Nanjing University of Science and Technology, Nanjing, China, in 2018.

He is currently a Lecturer with the School of Mechanical Engineering, Nanjing University of Science and Technology. His current research interests include servo control of mechatronic systems, hydraulic robot control, robust adaptive control, and nonlinear compensation.

YAOWEN GE received the B.Tech. degree from the School of Mechanical Engineering, Nanjing University of Science and Technology, Nanjing, China, in 2014, where he is currently pursuing the Ph.D. degree.

His current research interests include servo control of mechatronic systems, fault detection, and accommodation of dynamic systems.

JIANYONG YAO (Member, IEEE) received the B.Tech. degree from Tianjin University, Tianjin, China, in 2006, and the Ph.D. degree in mechatronics from Beihang University, Beijing, China, in 2012.

From October 2010 to October 2011, he was a Visiting Exchange Student with the School of Mechanical Engineering, Purdue University. He joined the School of Mechanical Engineering, Nanjing University of Science and Technology, Nanjing, China, in 2012, where he is currently a Full Professor. His current research interests include servo control of mechatronic systems, adaptive and robust control, fault detection, and accommodation of dynamic systems.

GUOLAI YANG received the Ph.D. degree in automatic weapons and ammunition engineering from the Nanjing University of Science and Technology, Nanjing, China, in 1999.

He visited the Department of Mechanical Engineering, Texas Tech University, Lubbock, as a Visiting Professor, in 2010. He is currently a Professor of mechanical engineering with the School of Mechanical Engineering. He also works as the Dean of the School of International Education, Nanjing University of Science and Technology. His research interests include theory and experimental method of time-varying mechanics, mechanical system dynamics, virtual design, and simulation technique.